JOURNAL OF MATERIALS SCIENCE 17 (1982) 2184–2193

Process design for the production of a ceramic-like body from recycled waste glass

Part 3 *The influence of microstructure and devitrification behaviour on the physical properties*

I. W. M. BROWN, K. J. D. MACKENZIE
Chemistry Division, Department of Scientific and Industrial Research, Private Bag, Petone, New Zealand

Comparison of the physical and microstructural properties for a number of specimens of a body derived from waste glass indicates that conventional empirical relationships are followed between the modulus of rupture and porosity derived from density measurements (porosities measured by water penetration cannot be used for this purpose because of the existence of extensive closed-pore systems in some samples). Conventional relationships between the modulus of rupture and mean grain size of the starting materials are also found to hold for these bodies. X-ray diffraction studies of the devitrification products formed during firing (cristobalite, devitrite and feldspars) showed that the concentrations of the crystalline phases depend on the clay binder content of the body, the firing temperature, soaking time and heating rate, but are independent of the other fabrication variables. Scanning electron microscopy shows that the cristobalite occurs as a crust around the poreholes, its relative concentration varying almost linearly with porosity. Feldspar is formed by reaction between the clay binder and the glass, with an activation energy similar to that for sodium diffusion in feldspar ($\sim 169\,kJ\,mol^{-1}$). Diffusion of sodium from the glass into the clay aggregates is apparently accompanied by a redistribution of silicon and aluminium in the aluminosilicate lattice, to maintain the charge balance.

1. Introduction

In Parts 1 and 2 of this paper [1, 2] it was shown that a ceramic-like material can be produced by sintering ground waste glass in the presence of a small amount of clay, which is added solely for the purpose of imparting a degree of green strength, but is also found to influence the sintering behaviour by modifying the viscosity and/or the surface tension of the glass particles [2]. Another process which was suspected of modifying the viscosity and thus changing the sintering behaviour is the formation of crystalline devitrification products in the glass particles [2]; this process may be assisted by interactions with the clay binder or any other inorganic material added as a mineralizer or colourant.

A most important property of a ceramic material is its fired strength, which, in the case of the present body, was correlated in a previous paper [2] with a number of fabrication variables in order to optimize the production process. Theories of strength development in ceramics [3] suggest that relationships should exist between strength and microstructural aspects such as porosity and grain size; a typical empirical relationship found to exist between the true porosity, P, and modulus of rupture, σ, of many ceramics has the form [3]

$$\sigma = \sigma_0 \exp(-bP), \quad (1)$$

where σ_0 is the modulus of rupture at zero porosity and b is a constant having a value of 3 to 11. In an attempt to put Equation 1 on a theoretical basis,

0022–2461/82/082184–10$03.70/0

Knudsen [4] equated the strength with the contact area between the particles, calculating the contact area between grains of unit volume as a function of porosity for three packing arrangements of spheres. The curves are linear at lower porosities, with slopes corresponding to b-values ranging from 6 for the most open packing to 9 for the most condensed packing.

In many ceramics, the relationship between the modulus of rupture, σ, and the mean grain size, G, can be expressed by [3]

$$\sigma = AG^{-a}, \quad (2)$$

where A and a are constants. If the grain size is assumed to be related to the Griffith flaw size, the value of a should be 0.5, provided the porosity is constant. In practice, values of a ranging from 0.17 to 0.55 have been found for a number of ceramics [3].

The aim of the present work was to investigate the influence of microstructural factors on the properties of the newly-developed waste glass body, and to study aspects of the chemistry of devitrification and crystalline phase formation during firing. The microstructural study was made by optical and scanning electron microscopy (SEM), the formation of devitrification products being investigated by qualitative and quantitative X-ray diffraction, SEM and energy dispersive X-ray analysis (EDAX) probe.

2. Experimental procedures

Microscopic examination of the surface-ground samples previously used for strength testing [2] was carried out in reflected light using a Nikon type 114 photomicroscope and by SEM. Identification of the crystalline phases in the fired body was made by X-ray examination of the flat ground surfaces, but for quantitative estimates of the major devitrification products (devitrite, $Na_2O \cdot 3CaO \cdot 6SiO_2$, cristobalite, SiO_2, and feldspar, $NaAlSiO_4$) the fired samples were powdered and 10% pre-calcined α-Al_2O_3 added as an internal standard. The relative heights of the diagnostic peaks were determined in preference to the areas, since the latter, estimated by scanning the appropriate angular range and counting the integrated number of pulses, were found to be less reliable due to the occurrence of several overlapping peaks in the diagnostic regions of these spectra. The peaks used for the estimation of the principal phases were the cristobalite peak at $d = 0.405$ nm, the devitrite peak at $d = 0.299$ nm and a feldspar peak at $d = 0.417$ nm, all referred to an alumina standard peak at $d = 0.348$ nm. The peak height ratios were not converted to phase percentages via calibration graphs, in view of the intractable problem of preparing a definitive devitrite calibration material; in any case, the purpose of this work, to investigate *changes* in phase composition under different fabrication conditions, was adequately served by the height ratio measurements.

3. Results and discussion

3.1. Influence of microstructure on strength

3.1.1. Strength against porosity

Equation 1, relating the modulus of rupture to the porosity of bodies having similar grain size, was developed as a phenomenological description of true porosity data derived from density measurements. Equation 1 has been shown to hold for earthenware bodies containing flint [5] (for which the slope, b, of the linear plot of $\ln \sigma$ against P (true) is 3.9), for alumina [4] (for which $b = 4$ for bending strength or 8 to 9 for compressive strength), and zirconia [4] (for which $b = 7$ for compressive strength). A similar relationship has been shown [6] to hold for Young's modulus of alumina as reported by a number of workers, all of which values lie on a line of slope 3.95. Although the porosity values used in the latter work [6] were again mainly true porosities, one set of data derived from measurements of apparent porosity was included, and found, perhaps fortuitously, to lie on the line [6]. The porosities reported in Part 2 of this paper [2] for the present glass body are apparent rather than true porosities; a plot of these porosities against the modulus of rupture values also reported in Part 2, while not necessarily expected to show the linear behaviour predicted by Equation 1, is nevertheless interesting from the point of view of its microstructural implications (Fig. 1).

Three regions can be distinguished in Fig. 1. In the low porosity region, a wide range of strength is recorded for samples of very similar porosity, while at intermediate porosities (3 to 18%), the strength is virtually independent of porosity. At higher porosities (20 to 30%) a marked deterioration of strength is observed with increasing porosity. An analogous plot of the modulus of elasticity, E, shows identical behaviour. All the specimens included in Fig. 1 were prepared from

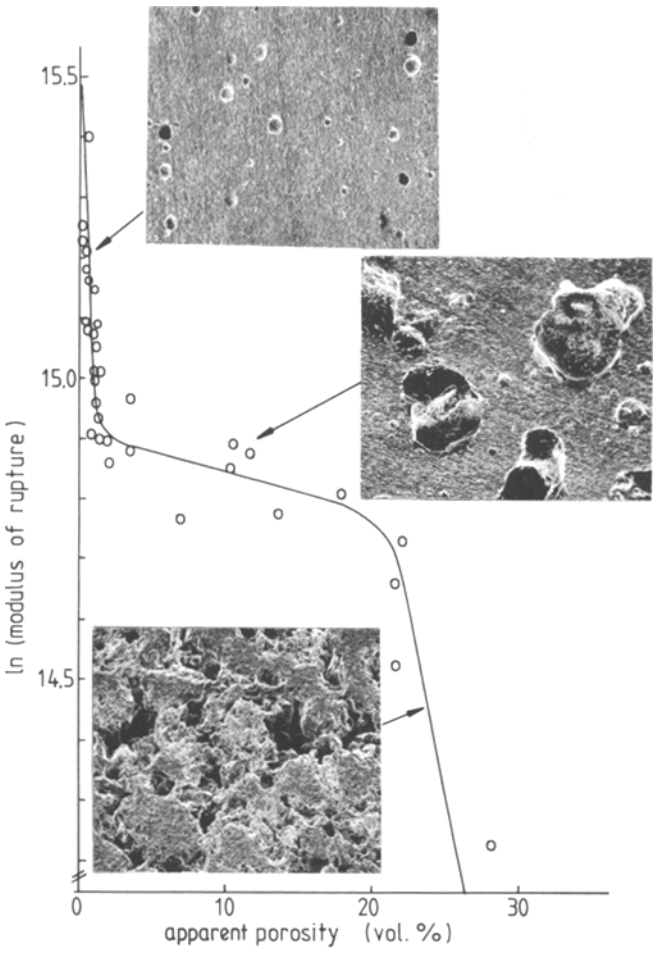

Figure 1 Relationship between modulus of rupture and porosity measured by the water penetration method. Insets show typical microstructures of the three regions of the curve (× 26 magnification).

glass powder of the same grain size distribution, the difference in porosity and strength being due to variations in the fabrication conditions. Microscopic examination of the polished samples shows that those falling in the high porosity–low strength region contain typically deep, connected pore craters, with angular grain boundaries visible (Fig. 1). Some specimens falling in this porosity range contain large numbers of small diameter pores while others show smaller numbers of larger diameter pores; in the latter, the matrix surrounding the pores appears better sintered and these samples also have higher strengths. In the region of intermediate porosity, all the samples are characterized by a high degree of sintering of the glassy matrix (Fig. 1), but deep, open pores are still visible, varying considerably in diameter from sample to sample. Thus, although the pore volume accessible to the measuring fluid varies considerably between samples, the strength is apparently more dependent on the integrity of the matrix, which is very similar in all these specimens. The low-porosity region is characterised by very few, small, open pores (Fig. 1), but in all these specimens there is evidence of considerable sub-surface porosity. In this region, therefore, the porosities measured by fluid penetration do not adequately represent the true porosity because of the existence of an extensive closed pore sub-system in many of these samples.

In view of these microstructural considerations, a test of the applicability of Equation 1 to the present body must be based on true porosity values derived from the measured densities (D) of the samples by

$$P(\text{true}) = (D_0 - D)/D_0, \qquad (3)$$

where D_0 is the density of a fully dense body.

Fig. 2 shows a plot of $\ln \sigma$ against porosity calculated by setting $D_0 = 2.52$ (this values makes allowance for the 10% halloysite in the body). Despite the scatter, Fig. 2 suggests that the

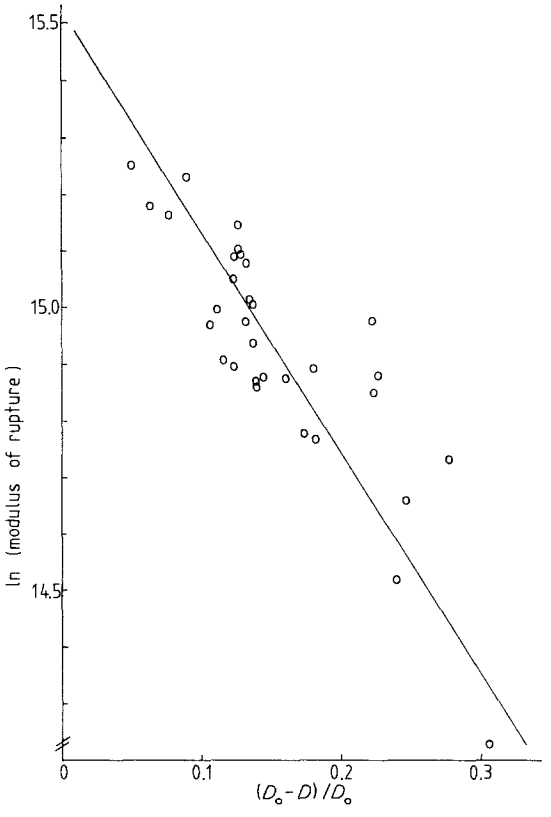

Figure 2 Relationship between modulus of rupture and fractional porosities calculated from density measurements for waste-glass bodies.

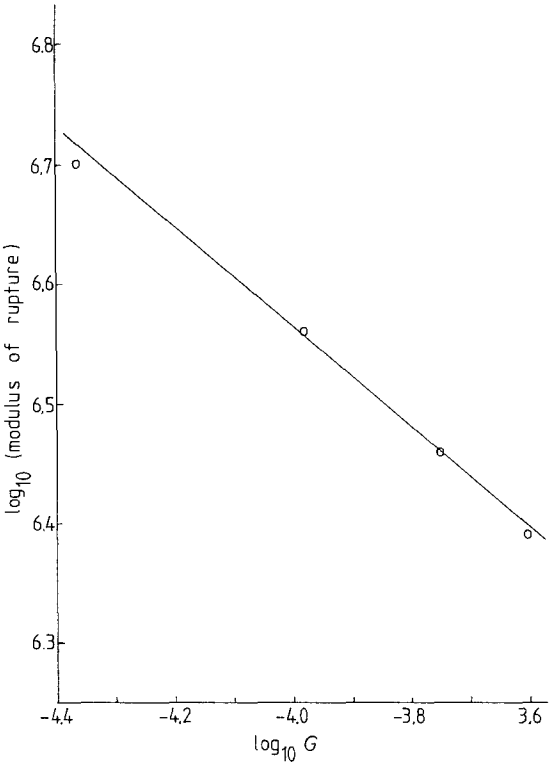

Figure 3 Relationship between modulus of rupture and mean grain size for waste-glass bodies.

expected linear relationship applies, from the slope of which $b = 3.98$. The complete porosity relationship can be expressed as

$$\sigma = 5.4 \times 10^6 \exp(-3.98P), \qquad (4)$$

where σ is in $kg\,m^{-2}$.

This value of b is very similar to that of Dinsdale and Wilkinson [5] for earthenware bodies, but the physical implications are not obvious because of the totally empirical nature of Equation 1.

Plots of the elastic moduli against calculated porosities show a linear relationship with greater scatter; b values estimated from these plots fall in the range 2 to 3.3. Again, the physical significance of the numerical value of b is not obvious.

3.1.2. Strength against grain size

The simple relationship between the strength of a ceramic body and its mean grain size (Equation 2) is strictly valid only for specimens of comparable porosity; where the porosity also varies with grain size, other equations have been proposed [4, 7] to take this into account. During the course of studies on the present body, a series of experiments were made using powders of different grain size distributions [2]. The measured porosities of these specimens indicated a range of porosities spanning about 13 vol%, but the porosities calculated according to Equation 3 were much more closely similar. On this basis, the use of Equation 2 appears to be justified, and the resulting plot of $\log_{10}\sigma$ against $\log_{10} G$ (Fig. 3) is linear, with a slope of 0.42.

An analogous plot of the elastic modulus, E, is less satisfactory, but indicates a slope of ~ 0.3. Although Griffith crack theory [3] suggests that the slope of this plot should have the value 0.5, the present values fall within the range found for a number of other ceramics. The possible theoretical implications of the present result are however obscured by the wide distribution of grain sizes present in these samples (the values of G used in Fig. 3 were the mean values taken from the particle size distribution curves). The similarity between the present values of a and those reported for other ceramic material may merely be fortuitous.

3.2. Devitrification in the glassy body

X-ray diffraction analysis indicates that varying degrees of devitrification occur in all specimens during firing. The principal crystalline products are cristobalite (SiO_2), devitrite ($Na_2O \cdot 3CaO \cdot 6SiO_2$) and various feldspars, the latter resulting from reaction between the glass and the clay binder. Estimates of the changes in the relative concentrations of the three principal crystalline products, made as a function of the various fabrication variables, showed no significant differences in the nature or relative concentrations of these phases resulting from variations of the particle size distribution of the starting material, the mixing water content or the pressing pressure. Increasing the concentration of the clay binder resulted in a significant increase in the cristobalite and feldspar contents, but the devitrite content was less influenced (see Fig. 4).

In Part 2 of this paper [2] it was shown that increasing the clay binder content caused a marked increase in the porosity of the body, that is an increase in the effective surface area. Further, the amount of hydroxyl water released will increase as the clay content increases. Our observation that increasing the clay content causes an increase in cristobalite is therefore consistent with the known ability of water vapour to promote cristobalite formation in silica [8]. This point is discussed more fully below.

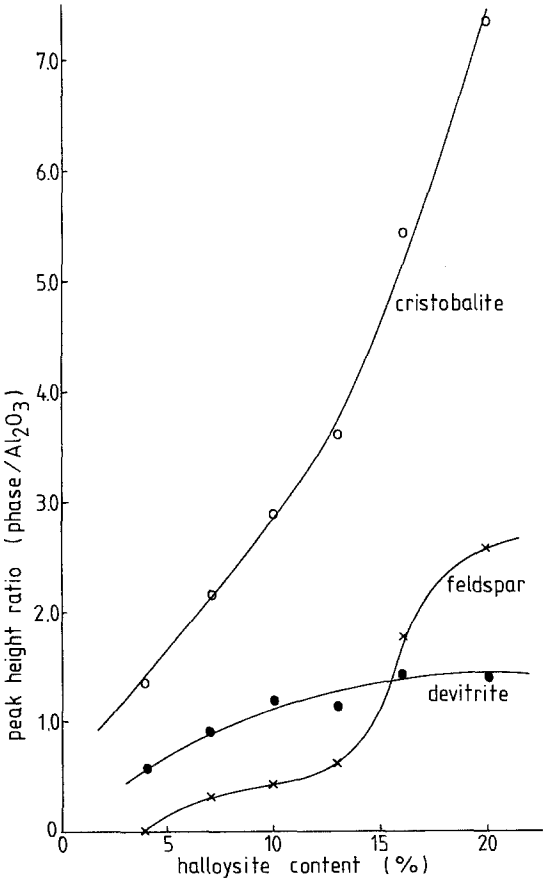

Figure 4 Development of crystalline phases in waste-glass bodies fired under standard conditions [2], as a function of halloysite binder content.

The increase in feldspar content results from the increase of available aluminium at higher clay contents, since scanning electron micrographs of the high-clay samples reveal spherical relicts of agglomerated clay particles, having a high Al content, and into which appreciable Na has also diffused (Fig. 5a). These regions, corresponding typically to feldspar compositions, are much less abundant in the lowest-clay samples.

Changing the soaking temperature was also found to significantly influence the formation of the crystalline phases (see Fig. 6).

The formation of maximum amounts of both cristobalite and feldspar occurs ~ 40° C lower than the temperature of maximum devitrite formation. Since the appearance of significant amounts of devitrite coincides with a decrease in both cristobalite and feldspar content, the devitrite-forming reaction apparently competes with cristobalite and feldspar for silica and Na_2O (or CaO) respectively. Studies of devitrite crystallization in pure soda-lime–silica glasses of similar composition having indicated maximum rates occurring variously at 955 [9] and 900° C [10]; the presence of other oxides such as MgO and Al_2O_3 has however been shown to influence the temperature at which the maximum rate of devitrite formation occurs [10]. On this basis, the presently observed temperature of maximum devitrite formation (~ 915° C) appears quite reasonable.

A similar but much less marked trend was observed in the relative proportions of the crystalline phases in samples held at the "standard" soaking temperature (915° C) for varying times (see Fig. 7).

At zero soaking times, the concentrations of cristobalite and feldspar were relatively high, but decreased with increasing soaking times, by contrast with devitrite formation, which increased slightly with increasing soaking times. These kinetic curves again indicate devitrite formation at the expense of cristobalite and feldspar.

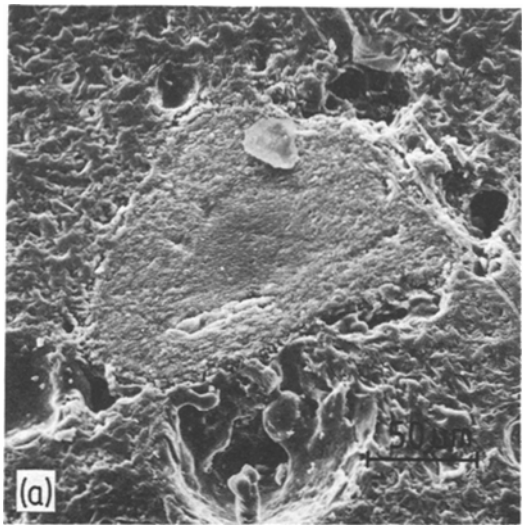

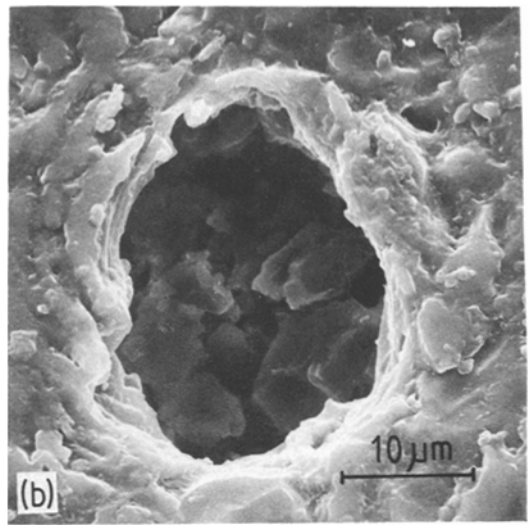

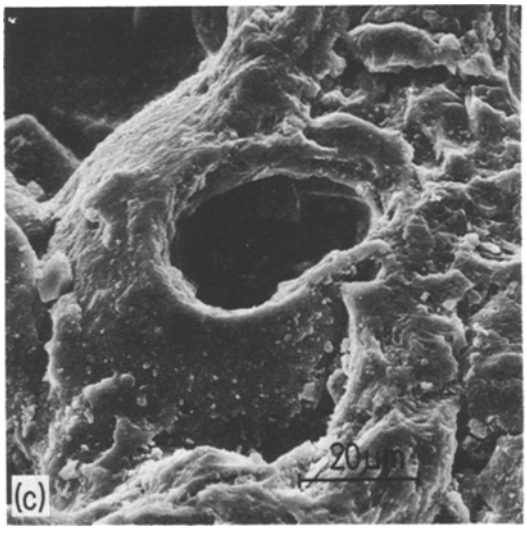

Figure 5 Scanning electron micrographs of waste-glass bodies, showing (a) a body containing 20% halloysite showing a spherical clay relict fully converted to a feldspar, (b) a typical void, surrounded by a cristobalite crust, and (c) a typical clay relict partially converted to feldspar, with associated cristobalite-encrusted voids.

Some unusual trends were also found in the series of specimens fired at different heating rates; although the relative proportions of the three principal crystalline phases showed little variation with heating rate, the X-ray diffraction trace of the sample fired at the lowest rate ($36^\circ C\,h^{-1}$) showed very marked development of other crystalline phases, principally Ca-rich feldspars, by contrast with the Na-feldspars occurring at higher heating rates. This may again reflect a kinetic effect arising from the slower diffusion of Ca into the aluminosilicate lattice (the diffusion coefficients of Ca and Na in feldspar glasses of albite composition at 915° C are 9.9×10^{-10} and $1.7 \times 10^{-5}\,cm^2\,sec^{-1}$ respectively [11]. The slower diffusion of Ca militates against the formation of Ca-feldspars at all but the slowest heating rates. The absence of Ca-feldspars in samples soaked for long periods at 915° C is probably due to the Ca-depleting effect of devitrite formation which is the favoured reaction at these higher temperatures. It has already been noted that the extensive formation of crystalline phases at slow heating rates interferes with glass particle sintering, resulting in decreased strength [2].

Another general phenomenon noted in the scanning electron micrographs of a range of specimens was the occurrence of a thick crust surrounding the pore holes (Fig. 5b). The EDAX probe showed this to contain only Si; these crusts are therefore composed of cristobalite, and, furthermore, represent the principal regions in which a purely siliceous phase was found. The preferential formation of cristobalite in the vicinity of pore holes suggests the participation of hydroxyl water originating from the clay binder, since it is via the interconnecting pore network that the diffusion of such water will occur following dehydroxylation. The nucleating effect of water vapour on cristobalite formation in vitreous silica is well known [8]. The relationship between pore holes and water vapour release is further confirmed by the SEM observation that the pores tend to occur in close proximity to the clay relicts which are the source of the hydroxyl water

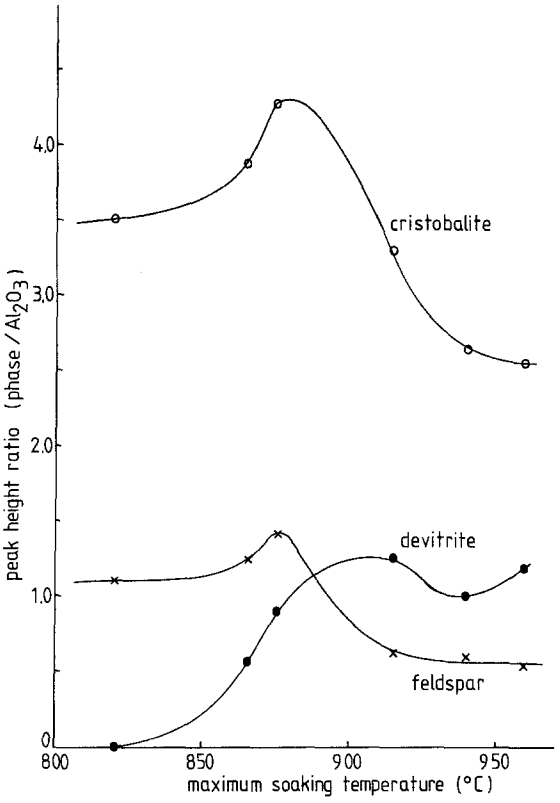

Figure 6 Development of crystalline phases in "standard" waste-glass bodies [2] as a function of maximum soaking temperature.

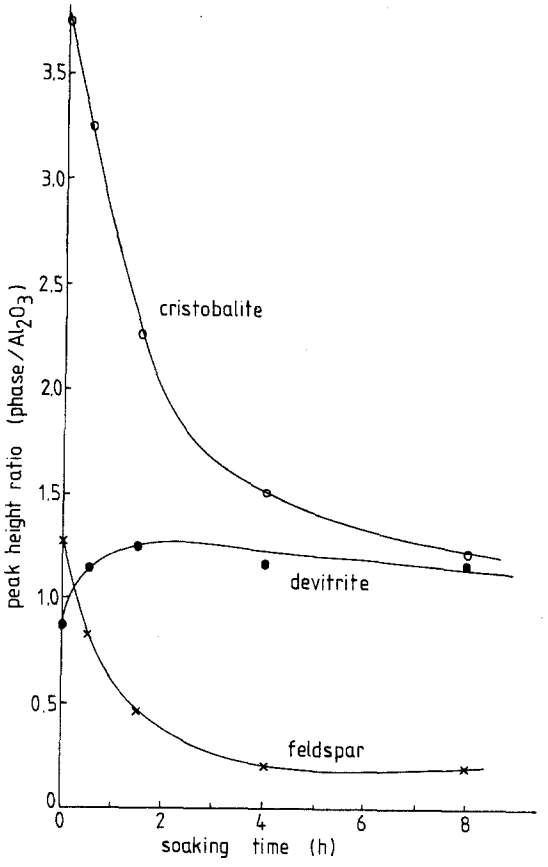

Figure 7 Development of crystalline phases in "standard" waste-glass bodies [2] as a function of soaking time at 915° C.

(Fig. 5c). On the basis of these observations, a general relationship might be expected between the porosity of the specimens and their crystalline silica and feldspar contents. Figs 8 and 9 show that such relationships appear to exist for cristobalite and feldspar provided the porosity values calculated from the measured densities are used.

Some of the scatter in the cristobalite plot will arise from the wide range of pore sizes observed to form in these materials. Since cristobalite formation is accelerated by the presence of water vapour and occurs in the region immediately adjacent to the pores, the high surface area of small pores will be more effective in promoting cristobalite crystal growth than the equivalent volume of large pores. Further, the observed scatter in the feldspar graph may arise in part from variation in the clay agglomerate size. Although the clay and glass were thoroughly intermixed, small localized agglomerates of up to 150 μm diameter could be seen by optical microscopy and SEM. As the rate of feldspar formation is shown in Section 3.3 to be controlled by sodium diffusion through the glass–clay interface into the clay agglomerate, variations in the volume of the clay agglomerates could cause considerable variation in the quantity of feldspar formed. No relationship between porosity and devitrite content was found, neither would one have been expected from the SEM observations.

3.3. Reactions between the glass grains and the clay binder

Optical and SEM examination of the larger aggregrates of clay binder found in the fired samples indicates in many cases an outer zone of different texture (Fig. 10a). The innermost material has the typically tubular morphology of unreacted halloysite, with no Na content detectable by EDAX, but having a Si–Al ratio of $\sim 2:1$, by contrast with a ratio of 1 : 1 for the identical unheated halloysite. The outer zone is generally of a more platy texture, with a significant Na content and a Si–Al ratio between 1 : 1 and 1 : 2. This zone

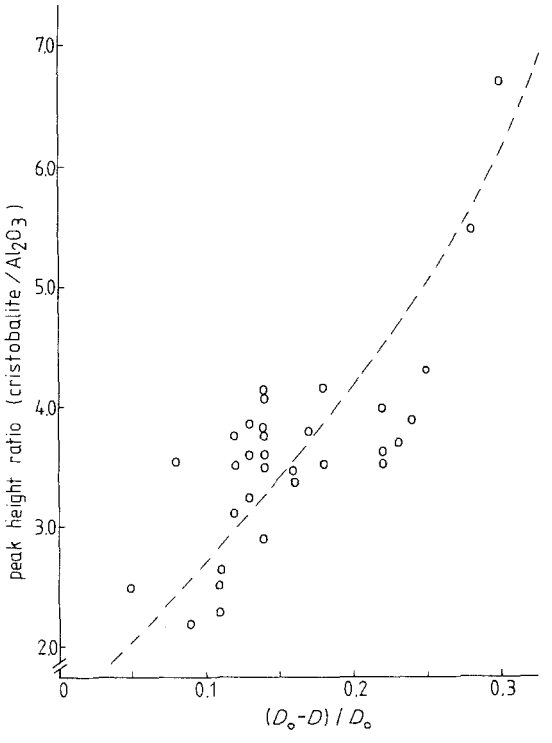

Figure 8 Relative cristobalite contents of waste-glass bodies as a function of fractional porosity calculated from density measurements.

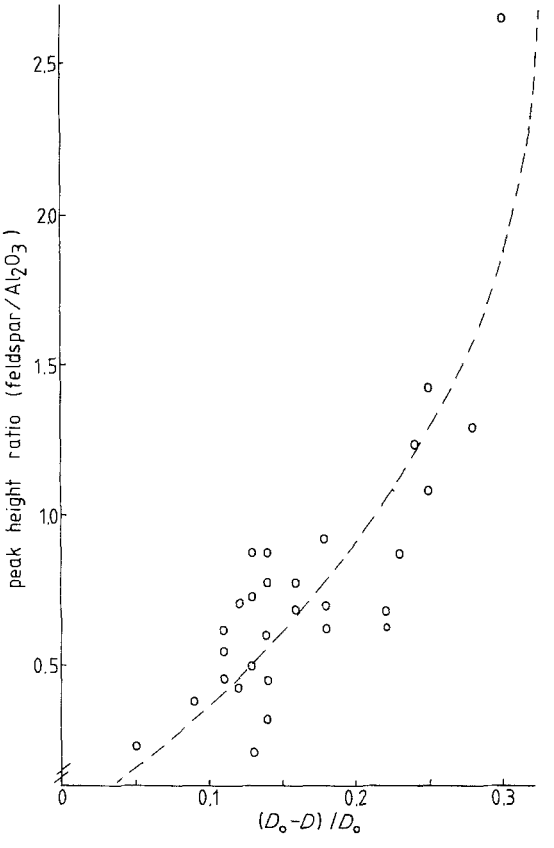

Figure 9 Relative Na-feldspar contents of waste-glass bodies as a function of fractional porosity calculated from density measurements.

corresponds to a Na-feldspar, and occurs very generally, except in the specimens fired at the lowest heating rates, in which Ca-containing feldspars are formed. Element density maps of a typical partially-reacted clay aggregate (Fig. 10b and c) show an enrichment of Al in the outer zone, the inner zone being enriched in Si. No significant migration of Ca into the aggregate was observed in this sample.

Since the texture of the material in the reacted zone is markedly different from that of the inner unreacted core, visual estimates of the degree of reaction could be made by microscopy for the series of samples fired at different soaking temperatures [2]. An Arrhenius plot of these data (Fig. 11) indicates an apparent activation energy of 169 kJ mol^{-1} for the process by which the feldspar phase is formed within the clay aggregates.

This activation energy is larger than that reported for the diffusion of Na into a feldspar glass of albite composition (56.5 kJ mol^{-1}) [12], but is of similar magnitude to energies reported by some workers for Na diffusion in crystalline albite feldspars (146–176 kJ mol^{-1}) [12]. A similar activation energy (about 209 kJ mol^{-1}) has also been reported [13] for the formation of the feldspars nepheline and carnegieite by reaction between mullite and $Na_2O \cdot 2SiO_2$ glass, a reaction which is probably also controlled by Na diffusion. Likewise, the kinetics of interaction between the clay binder and the glassy matrix of the present body appear to be controlled by Na diffusion. As the Na from the glassy matrix diffuses into the aluminosilicate aggregate, charge balance is maintained by re-distribution of Si and Al between the reacted and unreacted regions of the clay aggregate, as required by the stoichiometry of the particular feldspar product.

4. Conclusions

(1) In the present bodies derived from waste glass, a linear relationship is observed between ln (modulus of rupture) and the porosity, calculated from the measured densities of the specimens. The slope of this line (3.98) is similar to results reported for several other ceramic materials, but further conclusions cannot be drawn because of the purely empirical nature of this relationship. If porosity

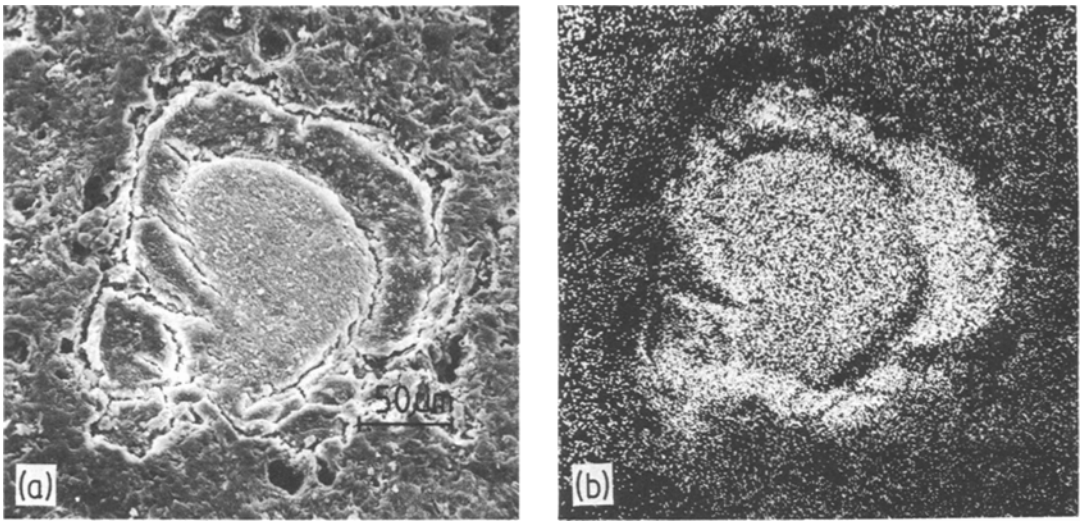

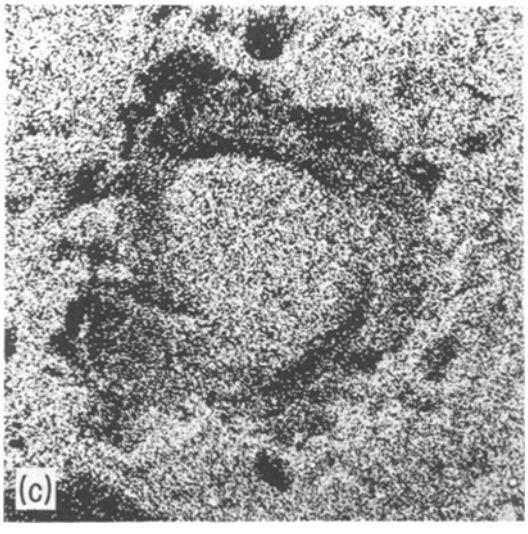

Figure 10 Scanning electron micrographs of a partially-reacted clay aggregate in a waste-glass body. (a) clay aggregate showing outer zone of Na-feldspar reaction product, (b) element density map for Al, and (c) element density map for Si.

values obtained by standard water penetration methods are similarly plotted, the resulting curve has three well-defined regions which have been shown by scanning electron microscopy to be related to the degree of matrix sintering and the development of a closed-pore system.

(2) A linear relationship is also observed between $\log_{10}$ (modulus of rupture) and $\log_{10}$ (mean grain size), for specimens fabricated from starting materials of different particle size distributions. The slope of this line (0.42) is similar to results reported for other ceramic materials, and is in reasonable agreement with the value of 0.5 predicted from Griffith crack theory.

(3) During firing, devitrification occurs in the glassy bodies with the formation of cristobalite, devitrite and feldspars, the latter resulting from reaction of the clay binder with the glass. The relative amounts of the various crystalline phases formed are independent of fabrication variables such as particle size distribution, mixing water content and pressing pressure, but are influenced by the clay binder content, maximum firing temperature, firing time and heating rate. The cristobalite occurs in all cases as a crust around the pore-holes; approximately linear relationships between the cristobalite and feldspar contents of the specimens and their porosity suggest that the formation of cristobalite is assisted by the nucleating action of the water which is formed during dehydroxylation of the clay binder and which escapes via poreholes which in general occur in close proximity to the clay relicts.

(4) The temperature dependence of feldspar-forming reactions between aggregates of clay binder and the glassy matrix has been measured by microscopic examination of the reaction zone thickness, and has a value similar to that for sodium diffusion in crystalline feldspars ($\sim$ 169 kJ mol^{-1}). This suggests that the rate of feldspar formation is controlled by the diffusion of sodium into the clay aggregate. Differences in the Si–Al ratio in the reacted and unreacted zones of the clay aggregates suggest that the reaction is also accompanied by re-distribution of silicon and aluminium, to maintain charge balance.

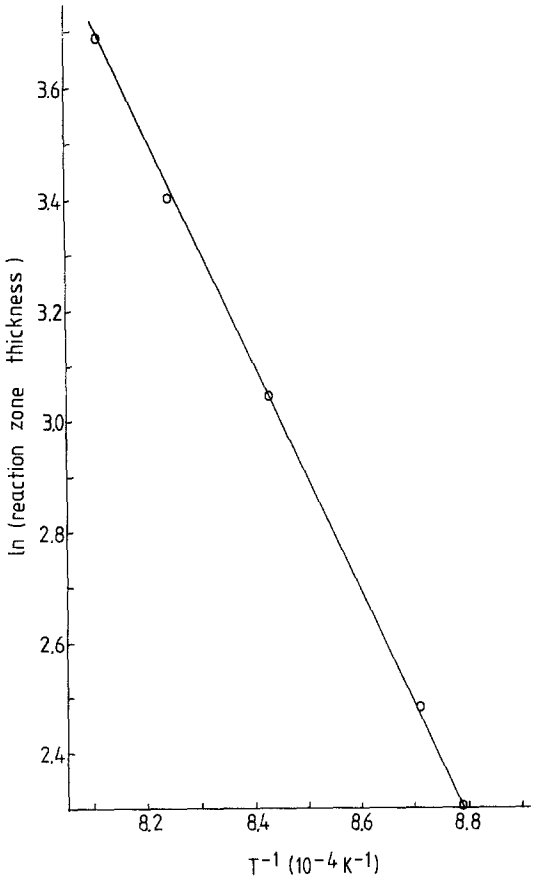

Figure 11 Arrhenius plot for formation of Na-feldspar in waste-glass body by reaction of the clay binder with the glassy matrix.

Acknowledgements

We are indebted to Mr R. M. Berezowski for technical assistance, and to Mr G. D. Walker for the scanning electron microscopy.

References

1. I. W. M. BROWN and K. J. D. MACKENZIE, *J. Mater. Sci.* **17** (1982) 2164.
2. *Idem, ibid.* **17** (1982) 2171.
3. J. E. BAILEY and N. A. HILL, *Proc. Brit. Ceram. Soc.* **15** (1970) 15.
4. F. P. KNUDSEN, *J. Amer. Ceram. Soc.* **42** (1959) 376.
5. A. DINSDALE and W. T. WILKINSON, *Proc. Brit. Ceram. Soc.* **6** (1960) 119.
6. F. P. KNUDSEN, *J. Amer. Ceram. Soc.* **45** (1962) 94.
7. E. M. PASSMORE, R. M. SPRIGGS and T. VASSILOS, *ibid.* **48** (1965) 1.
8. N. G. AINSLIE, C. R. MORELOCK and D. TURNBULL, in "Proceedings of the Symposium on Nucleation and Crystallization in Glass and Melts", Toronto, April 1961, edited by M. K. Reser (American Ceramic Society, Columbus, Ohio, 1962) p. 97.
9. A. J. MILNE, *J. Soc. Glass Technol.* **36** (1952) 275.
10. H. R. SWIFT, *J. Amer. Ceram. Soc.* **30** (1947) 171.
11. A. JAMBON and F. DELBOVE, *C.R. Hebd. Seances Acad. Sci., Ser. D* **284** (1977) 2191.
12. A. JAMBON and J. P. CARRON, *Geochim. Cosmochim. Acta* **40** (1976) 897.
13. K. INAGAKI and T. TORII, *Yogyo Kyokai Shi* **75** (1967) 70.

Received 7 September
and accepted 12 December 1981